AIAA JOURNAL
Vol. 34, No. 11, November 1996

Primal and Mixed Variational Principles for Dynamics of Spatial Beams

B. M. Quadrelli* and S. N. Atluri†
Georgia Institute of Technology, Atlanta, Georgia 30332-0356

A general formulation is presented for static and dynamic analysis of spatial elastic beams capable of undergoing finite rotations and small strains. The tangent maps associated to the finite rotation vector are used to compute the tangent iteration matrices used to integrate implicitly the equations of motion in descriptor form. A total Lagrangian primal corotational method and an updated Lagrangian mixed variational method are proposed to compute the tangent stiffness matrix. The tangent inertia matrices, including the gyroscopic and centrifugal terms, are also obtained by using the tangent maps of rotation. The numerical examples analyzed in this paper include static (pre- and postbuckling) and dynamic analysis of flexible beams structures. The new finite elements show a very good performance, in terms of fewer number of elements used and accuracy during the simulation, both for static and dynamic problems.

Nomenclature

A_i, a_i	= covariant base vectors at an arbitrary point of $\mathcal{S}_u$ and those at an arbitrary point of $\mathcal{S}_d$
A_ρ	= mass density
a_0	= $s\theta/\theta$
a_1	= $(1 - c\theta)/\theta^2$
a_2	= $(1/\theta^2)(1 - a_0)$
C_u, C_d	= undeformed and deformed configuration
$\boldsymbol{C}$	= skew-symmetric coupling term in the inertia matrix
c_1	= $(1/\theta^2)(a_0 - 2a_1)$
$\mathrm{d}t, \mathrm{d}Y^3$	= time differential and differential element of curve along the beam length
$d(\cdot), \delta(\cdot), \Delta(\cdot)$	= differential, virtual variation, and finite, but small, increment of a generalized coordinate
d_1	= $(1/\theta^2)(a_1 - 3a_2)$
$\boldsymbol{E}_i, \boldsymbol{e}_i$	= orthogonal basis (before and after rotation)
$F_1; F_3; E_1$	= variational functionals for elastodynamics of beams
$\boldsymbol{F}$	= deformation gradient tensor
$\mathcal{F}_{(\cdot)}$	= column vector the entries of which are the component base vectors of a right-handed triad
$g_0, g, \hat{g}$	= undeformed, deformed, and intermediate metric
$\boldsymbol{H}$	= angular momentum
$\boldsymbol{h}$	= vector of stretches
$\boldsymbol{I}_\rho$	= inertia tensor
J_α	= first moment of inertia
$J_{\alpha\beta}$	= second moment of inertia
$\boldsymbol{K}, \boldsymbol{k}, \tilde{\boldsymbol{k}}, l_3$	= initial and final curvature vectors
$\mathcal{L}$	= Lagrangian density
ℓ	= linear momentum
$\boldsymbol{M}$	= internal stress moment resultant
$\boldsymbol{q}$	= vector of generalized coordinates
$\boldsymbol{R}$	= rotation tensor
$\boldsymbol{S}_1$	= second Piola–Kirchoff stress tensor, $S_1^{kl}\boldsymbol{A}_k \otimes \boldsymbol{A}_l$
$\mathcal{S}_u, \mathcal{S}_d$	= undeformed and deformed cross section
$\mathcal{S}_{\sigma 0}(\mathcal{S}_{u0})$	= portion of the spatial boundary where tractions (displacements) are prescribed
$\boldsymbol{T}$	= internal stress resultants
$\boldsymbol{t}$	= first Piola–Kirchoff stress tensor, $t_1^{kl}\boldsymbol{A}_k \otimes \boldsymbol{a}_l$
$\boldsymbol{U}(\boldsymbol{V})$	= right (left) stretch tensor
$\mathcal{V}_0, \partial\mathcal{V}_0$	= volume and boundary of undeformed material element, defined by $\mathcal{S}_{\sigma 0} \cup \mathcal{S}_{u0}$, with $\mathcal{S}_{\sigma 0} \cap \mathcal{S}_{u0} = \emptyset$
$W_s(W_c)$	= strain energy (complementary strain energy) density per unit undeformed volume
Y^α	= curvilinear coordinates lying on the cross section
δ_{ij}	= Kronecker tensor
ε_{ijk}	= Levi–Civita or permutation tensor
ρ_0	= material density in C_u
$\varkappa$	= stress parameters
$\boldsymbol{\omega}$	= angular velocity vector
$(\cdot)_d, (\cdot)_\delta, (\cdot)_\Delta$	= differential, variation, and finite increment of a quasicoordinate
$(\cdot)_{,3}$	= covariant derivative with respect to Y^3 in C_u (using the g_0 metric)
$\boldsymbol{1}$	= identity matrix
$\times$	= cross (or vector) product
$\cdot$	= inner or dot or scalar product
$\otimes$	= tensor product operator
$:$	= double contraction of two second-order tensors [i.e., $\boldsymbol{A} : \boldsymbol{B} = A_{ij}B^{ij} = \mathrm{trace}(\boldsymbol{A} \cdot \boldsymbol{B}^T)$]
∇	= gradient operator along the vectors $\boldsymbol{g}^j$ associated with the curvilinear coordinates $\xi^i, \boldsymbol{g}^j(\partial/\partial\xi^i)$

Received Feb. 5, 1996; presented as Paper 96-1594 at the AIAA/ASME/ASCE/AHS/ASC 37th Structures, Structural Dynamics, and Materials Conference, Salt Lake City, UT, April 15–17, 1996; revision received June 11, 1996; accepted for publication June 12, 1996.

*Ph.D. Candidate, School of Aerospace Engineering. Member AIAA.
†Institute Professor and Regents' Professor of Engineering, Computational Modeling Center. Fellow AIAA.

I. Introduction

THIS paper deals with the modeling of the spatial static and dynamic behavior of homogeneous, isotropic, and linear elastic one-dimensional deformable bodies (beams or rods) undergoing arbitrarily large rotations and translations and small strains. The applications intended for this study are in multibody dynamics. Therefore, the spatial beam may be connected to other beams by means of holonomic constraints to form a multiflexible body mechanical system. In this paper, we will only deal with geometrical nonlinearities of flexible structural members that can be represented as beams. A sequel to this paper will study the multibody aspect of this problem. The first influential work on geometrically nonlinear static and dynamic analysis of three-dimensional finite strain beams, including arbitrarily large rotations, was that of Simo and Vu-Quoc.[1] A consistent variational approach for multiflexible body dynamics with beams was first presented by Cardona and Geradin.[2] In their work, they used the principle of virtual work and methods of nonlinear

structural dynamics to devise an incremental/iterative procedure to integrate the tangent equations of motion of a nonlinear beam. The first functional for finitely deformed beams, obtained in a consistent fashion from a general three-field mixed variational principle, was proposed by Iura and Atluri.[3,4] An exhaustive description of the topic of finite rotations is given in Argyris[5] and Pietraszkiewicz and Badur,[6] for applications in continuum mechanics as well as in plates and shells in Atluri,[7] for displacement-based variational formulations of nonlinear elastic beams in Cardona and Geradin,[2] for mixed variational principles of nonlinear elastic beams in Iura and Atluri,[3,4] in a unified manner in Atluri and Cazzani,[8] and for rigid-body dynamics in Borri et al.[9] Therefore, this paper is organized as follows. First, we overview the basic kinematics and kinetics of the problem. Second, we describe primal and dual variational functionals valid for nonlinear elastodynamics of three-dimensional continua, and then we specialize them to the case of a space beam. For additional details of the derivation, we refer the reader to Quadrelli.[10] Third, we derive the inertia, gyroscopic, and centrifugal matrices obtained from the inertia forces. Fourth, we derive the elastic tangent stiffness matrix and residual vector for a space beam with two different approaches: a primal, total Lagrangian (TL), corotational approach and a mixed, updated Lagrangian (UL) approach. Finally, we present some numerical results and the conclusions of this paper. In this paper, italic symbols and Greek letters denote scalar quantities, lowercase boldfaced letters denote vectors, capital boldfaced letters denote tensors, and boldfaced Greek letters usually denote vectors and sometimes tensors.

II. Basic Kinematics and Kinetics of a Beam Element

Consider a deformable one-dimensional continuum that is capable of undergoing large displacements and arbitrarily large rotations. To a material element in the undeformed configuration C_u, we assign the triad of basis vectors denoted by $\boldsymbol{E}_i$. To the same material element, but in the deformed configuration C_d, we assign the triad of basis vectors $\boldsymbol{e}_i$, which denotes $\boldsymbol{E}_i$ after a purely rigid-body rotation. The convected coordinates Y^i, with $i = 1, 2, 3$, denote a curvilinear system associated to a point centered in the material element. The displacement vector $\boldsymbol{u}$ describes the total displacement of the material element, the position of which, in C_u, is denoted by $\boldsymbol{X}$. The rotation tensor $\boldsymbol{R}$ describes the rigid-body rotation of the material element and can be parameterized as a function of the finite rotation vector $\boldsymbol{\alpha} = \theta\boldsymbol{e}$, where $\boldsymbol{e}$ is the unit vector fixed in space, and around which the finite rotation θ takes place. We have[9] the Euler–Rodrigues formula for the rotation tensor $\boldsymbol{R}$ and the associated tensor $\boldsymbol{\Gamma}$:

$$\begin{aligned}\boldsymbol{R}(\boldsymbol{\alpha}) &= \mathbf{1} + a_0(\boldsymbol{\alpha}\times\mathbf{1}) + a_1[\boldsymbol{\alpha}\times(\boldsymbol{\alpha}\times\mathbf{1})]\\ \boldsymbol{\Gamma}(\boldsymbol{\alpha}) &= \mathbf{1} + a_1(\boldsymbol{\alpha}\times\mathbf{1}) + a_2[\boldsymbol{\alpha}\times(\boldsymbol{\alpha}\times\mathbf{1})]\end{aligned} \tag{1}$$

For extended derivations of the kinematics of rotation, in rigid-body dynamics and in continuum mechanics, we refer the reader to Atluri and Cazzani.[8] In this work, we have decided to use $\boldsymbol{\alpha}$ in a consistent effort to extend to multiflexible body dynamics the work done by Borri et al.[9] in the context of multirigid-body dynamics. Following the assumptions of traditional (nonpolar) rod theory, we may postulate that the configuration of the beam is completely known when the inertial position of one point P of the cross section S and the orientation of the cross section itself with respect to a reference triad are known. A virtual variation of rotation can be expressed as $\boldsymbol{\varphi}_\delta\times\mathbf{1} = \delta\boldsymbol{R}\cdot\boldsymbol{R}^T$. Similarly, the angular velocity vector $\boldsymbol{\omega}$ can be written as $\boldsymbol{\omega}\times\mathbf{1} = \dot{\boldsymbol{R}}\cdot\boldsymbol{R}^T$ and similarly for the curvature vector $\boldsymbol{l}_3$, which may be represented as $\boldsymbol{l}_3\times\mathbf{1} = \boldsymbol{R}_{,3}\cdot\boldsymbol{R}^T$. In Borri et al.,[9] it is shown that the following representation holds for the angular velocity: $\boldsymbol{\omega} = \boldsymbol{\Gamma}(\boldsymbol{\alpha})\dot{\boldsymbol{\alpha}}$. If $\boldsymbol{\varphi}_\delta = \boldsymbol{\Gamma}(\boldsymbol{\alpha})\delta\boldsymbol{\alpha}$ represents the variation of rotation, then, for any arbitrary vector field $\boldsymbol{b}$, the associated tangent rotational maps may be derived in a straightforward manner.[9] The explicit expression for the tangent map associated with $\boldsymbol{\Gamma}^T$, namely $\boldsymbol{L}_{\Gamma^T}(\boldsymbol{\alpha},\boldsymbol{b})$, is

$$\begin{aligned}\delta\boldsymbol{\Gamma}^T\cdot\boldsymbol{b} &= \{-a_1(\boldsymbol{b}\times\mathbf{1}) + a_2[(\boldsymbol{\alpha}\times\boldsymbol{b})\times\mathbf{1} + \boldsymbol{\alpha}\times(\boldsymbol{b}\times\mathbf{1})]\\ &\quad + c_1(\boldsymbol{b}\times\mathbf{1})\cdot(\boldsymbol{\alpha}\otimes\boldsymbol{\alpha}) - d_1[(\boldsymbol{\alpha}\times\boldsymbol{b})\times\mathbf{1}]\cdot(\boldsymbol{\alpha}\otimes\boldsymbol{\alpha})\}\cdot\delta\boldsymbol{\alpha}\\ &= \boldsymbol{L}_{\Gamma^T}(\boldsymbol{\alpha},\boldsymbol{b})\cdot\delta\boldsymbol{\alpha}\end{aligned} \tag{2}$$

In the incremental formulation, the operator Δ may describe a material increment, a virtual variation, a total derivative (for example, a time derivative), or a covariant derivative [for example, the $(\cdot)_{,3}$ derivative].

A. Basic Kinematics

Next, we refer to Fig. 1. We assume that the beam cross section does not deform in its own plane or that the stress components in the plane of the cross section are zero. This implies that arbitrarily large strains are precluded, and we confine ourselves to the case of small strains and no warping, so that only shear deformation is allowed. For a material element of the beam, and following Iura and Atluri,[4] we may write that the global displacement vector is $\boldsymbol{v} = \boldsymbol{u} + Y^\alpha\cdot(\boldsymbol{e}_\alpha - \boldsymbol{E}_\alpha)$ and that the total global position vector of a reference point of the cross section is $\boldsymbol{x} = \boldsymbol{X} + \boldsymbol{v}$. The components of the stretch vector are $h^j = (R_{ij}/g)(\delta^i_3 + u^i_{,3}) - \delta^j_3$, the components of the curvature vector are $k^i = \frac{1}{2}\varepsilon_{ijk}R_{mj,3}R_{mk}$. We also have that $\boldsymbol{E}_{i,3} = \boldsymbol{K}\times\boldsymbol{E}_i$ and $\boldsymbol{e}_{i,3} = \boldsymbol{k}\times\boldsymbol{e}_i$. Some manipulation with these equations leads to $\delta\boldsymbol{\varphi}_{,3} = \delta\boldsymbol{l}_3 + \boldsymbol{l}_3\times\delta\boldsymbol{\varphi}$, which expresses the noncommutativity of the $\delta(\cdot)$ and the $(\cdot)_{,3}$ operators when quasi-coordinates are involved. More details on the kinematics may be found in Quadrelli.[10]

B. Basic Kinetics

We describe the inertial properties of the motion with a Lagrangian approach. This means that, contrary to rigid-body dynamics, in which the rotational motion is referred to the body triad, we refer the rotational motion to a fixed triad in space. In this approach, a material element labeled with the generalized coordinate vector $\boldsymbol{q} = (\boldsymbol{u},\boldsymbol{\alpha})^T$ is endowed with a Lagrangian density the structure of which we assume to be of the form $\mathcal{L} = \mathcal{T}(t,\boldsymbol{q},\dot{\boldsymbol{q}}) - f_1(\boldsymbol{v},R,U,t)$, where $\mathcal{T}$ is the kinetic energy density and f_1 is the mixed functional density described later in more detail. As required by the principle of

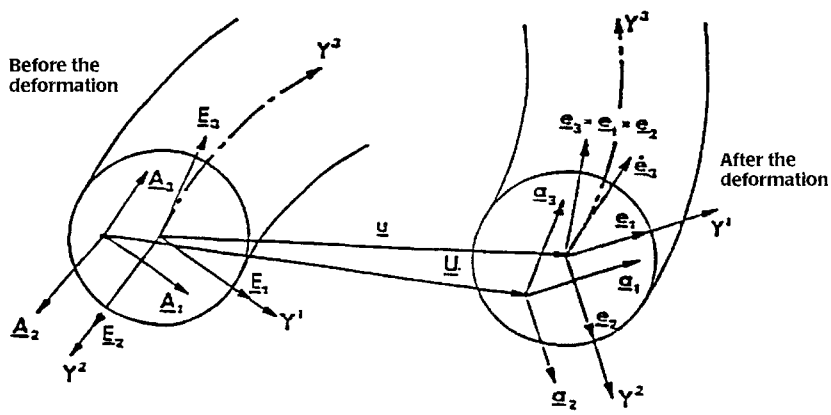

Fig. 1 Kinematics of beam deformation.

frame indifference, W_s can be a function of the deformation gradient $\boldsymbol{F}$ only through the right stretch tensor $\boldsymbol{U}$ [i.e., $W_s \equiv W_s(\boldsymbol{F}^T \cdot \boldsymbol{F})$]. An explicit expression for W_s may be found in Iura and Atluri.[4] In our derivation, we make the assumption that the material is linearly elastic and that the system is scleronomic; i.e., the kinetic energy density is independent of time. Then, our derivation is based on the functional

$$E_1 = \int_{[t_i, t_{i+1}]} \left\{ \int_{\mathcal{V}_0} \mathcal{T}(\boldsymbol{q}, \dot{\boldsymbol{q}})\, \mathrm{d}V - F_1(\boldsymbol{v}, \boldsymbol{R}, \boldsymbol{U}, \boldsymbol{t}) \right\} \mathrm{d}t \tag{3}$$

1. Four-Field Principle

A four-field mixed principle valid for a general elastic material, involving $\boldsymbol{v}, \boldsymbol{R}, \boldsymbol{U}$, and $\boldsymbol{t}$ as independent variables, may be stated as the stationarity condition of this functional:

$$\begin{aligned} &F_1(\boldsymbol{v}, \boldsymbol{R}, \boldsymbol{U}, \boldsymbol{t}) \\ &= \int_{\mathcal{V}_0} \left\{ W_s(\boldsymbol{U}) + \boldsymbol{t}^T : [(\boldsymbol{I} + \operatorname{grad} \boldsymbol{v}) - \boldsymbol{R} \cdot \boldsymbol{U}] - \rho_0 \boldsymbol{b} \cdot \boldsymbol{v} \right\} \mathrm{d}V \\ &- \int_{\mathcal{S}_{\sigma t}} \bar{\boldsymbol{t}} \cdot \boldsymbol{v}\, \mathrm{d}A - \int_{\mathcal{S}_{u0}} \boldsymbol{N} \cdot \boldsymbol{t} \cdot (\boldsymbol{v} - \bar{\boldsymbol{v}})\, \mathrm{d}A \end{aligned} \tag{4}$$

where $\boldsymbol{b} = \bar{\boldsymbol{f}}, \bar{\boldsymbol{f}}$ denotes applied body forces per unit mass; $\bar{\boldsymbol{t}}$ is the prescribed tractions on $\mathcal{S}_{\sigma 0}$, and $\bar{\boldsymbol{v}}$ is the prescribed displacements on $\mathcal{S}_{u0}$. In F_1, $\boldsymbol{v}$ must be C^0 continuous, $\boldsymbol{R}$ orthogonal, $\boldsymbol{U}$ symmetric, and $\boldsymbol{t}$ unsymmetric, to be admissible trial fields. When the condition $\delta F_1 = 0$ is enforced for arbitrary and independent variations such as C^0 continuous $\delta \boldsymbol{u}, \delta \boldsymbol{R}$ under the constraint $\delta \boldsymbol{R} \cdot \boldsymbol{R}^T = (\delta \boldsymbol{R} \cdot \boldsymbol{R}^T)_a$, symmetric $\delta \boldsymbol{U}$, and unsymmetric $\delta \boldsymbol{t}$, the following Euler–Lagrange equations (ELE) are obtained: constitutive law (CL), $\partial W_s / \partial \boldsymbol{U} = \frac{1}{2}(\boldsymbol{t} \cdot \boldsymbol{R} + \boldsymbol{R}^T \cdot \boldsymbol{t}^T) = (\boldsymbol{t} \cdot \boldsymbol{R})_s$; compatibility condition (CC), $(\boldsymbol{I} + \operatorname{grad} \boldsymbol{v}) = \boldsymbol{R} \cdot \boldsymbol{U}$; angular momentum balance (AMB), $(\boldsymbol{t}^T \cdot \boldsymbol{U} \cdot \boldsymbol{R}_a^T) = \boldsymbol{0}$; linear momentum balance (LMB), $\nabla_0 \cdot \boldsymbol{t} + \rho_0 \boldsymbol{b} = \boldsymbol{0}$; together with the natural boundary conditions, traction boundary condition (TBC), $\boldsymbol{N} \cdot \boldsymbol{t} = \bar{\boldsymbol{t}}$ on $\mathcal{S}_{\sigma 0}$, and displacement boundary condition (DBC), $\boldsymbol{v} = \bar{\boldsymbol{v}}$ on $\mathcal{S}_{u0}$.

2. Three-Field Principle

It is possible to derive a complementary variational principle involving $\boldsymbol{v}, \boldsymbol{R}$, and $\boldsymbol{t}$ alone. This can be done if $\boldsymbol{U}$ is eliminated from F_1 by applying the following contact (Legendre) transformation:

$$W_s(\boldsymbol{U}) + W_c(\boldsymbol{r}) = \tfrac{1}{2}(\boldsymbol{t} \cdot \boldsymbol{R} + \boldsymbol{R}^T \cdot \boldsymbol{t}^T) : \boldsymbol{U} \tag{5}$$

where $\boldsymbol{r} = \frac{1}{2}(\boldsymbol{t} \cdot \boldsymbol{R} + \boldsymbol{R}^T \cdot \boldsymbol{t}^T)$ is the symmetrized Biot–Lur'e stress tensor or Jaumann stress tensor, and W_c is the called complementary energy density. Physically, the Jaumann stress is the stress tensor associated with the force vector acting on the stretched, but not yet rotated, differential element of area, and measured per unit of undeformed area. Making use of this contact transformation is equivalent to adopting the hypothesis that CL, $\partial W_c / \partial \boldsymbol{r} = \boldsymbol{U}$ is a priori met. When the equation for this contact transformation is substituted into the expression of functional F_1, the following Hellinger–Reissner type three-field functional is obtained:

$$\begin{aligned} F_3(\boldsymbol{v}, \boldsymbol{R}, \boldsymbol{t}) &= \int_{\mathcal{V}_0} \left\{ -W_c\left[\tfrac{1}{2}(\boldsymbol{t} \cdot \boldsymbol{R} + \boldsymbol{R}^T \cdot \boldsymbol{t}^T)\right] \right. \\ &\left. + \boldsymbol{t}^T : (\boldsymbol{I} + \operatorname{grad} \boldsymbol{v}) - \rho_0 \boldsymbol{b} \cdot \boldsymbol{v} \right\} \mathrm{d}V \\ &- \int_{\mathcal{S}_{\sigma 0}} \bar{\boldsymbol{t}} \cdot \boldsymbol{v}\, \mathrm{d}A - \int_{\mathcal{S}_{u0}} \boldsymbol{N} \cdot \boldsymbol{t} \cdot (\boldsymbol{v} - \bar{\boldsymbol{v}})\, \mathrm{d}A \end{aligned} \tag{6}$$

To be admissible, the independent fields in functional F_3 have to satisfy the following requirements: $\boldsymbol{v}$ must be C^0 continuous, $\boldsymbol{R}$ orthogonal, and $\boldsymbol{t}$ unsymmetric. When the condition $\delta F_3 = 0$ is imposed for arbitrary and independent $\delta \boldsymbol{v}$, $\delta \boldsymbol{R}$, and $\delta \boldsymbol{t}$, subject only to the additional constraint $(\boldsymbol{R} \cdot \delta \boldsymbol{R}^T)_s = \boldsymbol{0}$, the following ELE are recovered: CC, $\boldsymbol{R} \cdot (\partial W_c / \partial \boldsymbol{r})_s = (\boldsymbol{I} + \operatorname{grad} \boldsymbol{v})$; AMB, $[\boldsymbol{R} \cdot (\partial W_c / \partial \boldsymbol{r})_s \cdot \boldsymbol{t}]_a = \boldsymbol{0}$; LMB, $\nabla_0 \cdot \boldsymbol{t} + \rho_0 \boldsymbol{b} = \boldsymbol{0}$; together with the natural boundary conditions TBC, $\boldsymbol{N} \cdot \boldsymbol{t} = \bar{\boldsymbol{t}}$ on $\mathcal{S}_{\sigma 0}$, and DBC, $\boldsymbol{v} = \bar{\boldsymbol{v}}$ on $\mathcal{S}_{u0}$. A property of the functional F_3 (or of F_1 before the contact transformation) is that one of its ELE is the AMB for the first Piola–Kirchoff stress tensor. This AMB is therefore embedded in the complementary energy density defined in terms of the Jaumann stresses. The Jaumann stress is an objective stress measure, which is useful in finite deformation elasticity.

3. F_1 Functional for a Beam

Considering now the stress, we can write that the internal virtual work (IVW)[7] can be expressed as

$$IVW = \int_{\mathcal{V}} \boldsymbol{t} : \delta \boldsymbol{F}^T\, \mathrm{d}V$$

The unit normal in C_u is $\boldsymbol{N} = g_0 \boldsymbol{A}^3 = \boldsymbol{E}_3$. Defining the internal stress resultants and moments as

$$\boldsymbol{T} = \int g_0 \boldsymbol{A}^3 \cdot \left(\boldsymbol{S}_1 \cdot \boldsymbol{F}^T\right) \mathrm{d}A$$

and

$$\boldsymbol{M} = \int Y^\alpha \boldsymbol{e}_\alpha \times \left[g_0 \boldsymbol{A}^3 \cdot \left(\boldsymbol{S}_1 \cdot \boldsymbol{F}^T\right)\right] \mathrm{d}A$$

respectively, the IVW can be written as

$$IVW = \int_L [\boldsymbol{T} \cdot \delta^o \boldsymbol{h} + \boldsymbol{M} \cdot \delta^o \boldsymbol{\kappa}]\, \mathrm{d}Y^3 \tag{7}$$

where $\delta^o \boldsymbol{h} = \delta \boldsymbol{u}_{,3} - \boldsymbol{\varphi}_\delta \times (\boldsymbol{X} + \boldsymbol{u})_{,3} = \boldsymbol{R} \cdot \delta \boldsymbol{h}$ is the corotational variation of the stretch vector, and $\delta^o \boldsymbol{\kappa} = \boldsymbol{\varphi}_{\delta,3} = \delta \boldsymbol{l}_3$ is the corotational variation of the curvature vector. With the notation just used, we may specialize the functional F_1 for the beam as[4]

$$\begin{aligned} &F_1(\boldsymbol{u}, \boldsymbol{R}, \boldsymbol{h}, \tilde{\boldsymbol{k}}, \boldsymbol{T}, \boldsymbol{M}) \\ &= \int_{\mathcal{V}} [W_s(\boldsymbol{h}, \tilde{\boldsymbol{k}}) + \boldsymbol{T} \cdot \{(\boldsymbol{X} + \boldsymbol{u})_{,3} - \boldsymbol{R} \cdot (\boldsymbol{h} + \boldsymbol{E}_3)\} \\ &+ \boldsymbol{M} \cdot \{\boldsymbol{l}_3 - \boldsymbol{R} \cdot \tilde{\boldsymbol{k}}\} - \boldsymbol{q} \cdot \boldsymbol{u}]\, \mathrm{d}L - {}_{\mathcal{S}^\sigma}[\bar{\boldsymbol{q}} \cdot \boldsymbol{u}]_{Y^3 = 0}^{Y^3 = L_d} \\ &- {}_{\mathcal{S}^u}[\boldsymbol{T} \cdot (\boldsymbol{u} - \boldsymbol{u}) + \boldsymbol{M} \cdot (\boldsymbol{\varphi} - \bar{\boldsymbol{\varphi}})]_{Y^3 = 0}^{Y^3 = L_d} \end{aligned} \tag{8}$$

where the terms involving the contributions of the distributed moment have been neglected (this is because distributed moments may be shown to lead to a nonconservative load). After taking the variation, we obtain the following: CL, $(\partial W_s / \partial \boldsymbol{h}) - \boldsymbol{T} \cdot \boldsymbol{R} = \boldsymbol{0}$ and $(\partial W_s / \partial \tilde{\boldsymbol{k}}) - \boldsymbol{M} \cdot \boldsymbol{R} = \boldsymbol{0}$; CC, $(\boldsymbol{X} + \boldsymbol{u})_{,3} - \boldsymbol{R} \cdot (\boldsymbol{h} + \boldsymbol{E}_3) = \boldsymbol{0}$ and $\boldsymbol{l}_3 - \boldsymbol{R} \cdot \tilde{\boldsymbol{k}} = \boldsymbol{0}$; LMB, $\boldsymbol{T}_{,3} + \boldsymbol{q} = \boldsymbol{0}$; and AMB, $\boldsymbol{M}_{,3} + (\boldsymbol{X} + \boldsymbol{u})_{,3} \times \boldsymbol{T} = \boldsymbol{0}$; and the boundary conditions $\bar{\boldsymbol{q}} - \boldsymbol{T} = \boldsymbol{0}$ and $\boldsymbol{M} = \boldsymbol{0}$ on $\mathcal{S}^\sigma$ and $\boldsymbol{u} - \bar{\boldsymbol{u}} = \boldsymbol{0}$ and $\boldsymbol{\varphi} - \bar{\boldsymbol{\varphi}} = \boldsymbol{0}$ on $\mathcal{S}^u$.

4. F_3 Functional for a Beam

In a completely equivalent way, from F_3 we obtain its variation δF_3, which leads to the same Euler–Lagrange equations as the F_1 functional, but in which the strains and curvature measures are no longer present. The contact transformation is allowed because the constitutive equation is invertible. The contact transformation then takes the following form:

$$W_s + W_c = \boldsymbol{T} \cdot (\boldsymbol{R} \cdot \boldsymbol{h}) + \boldsymbol{M} \cdot (\boldsymbol{R} \cdot \tilde{\boldsymbol{k}}) \tag{9}$$

5. Kinetic Energy for a Beam

For a material element of the beam, the kinetic energy may be written as

$$T = \frac{1}{2} \int_{\mathcal{V}} \rho \dot{\boldsymbol{v}} \cdot \dot{\boldsymbol{v}}\, \mathrm{d}V = \frac{1}{2} \int_{\mathcal{L}} (\boldsymbol{\ell} \cdot \dot{\boldsymbol{u}} + \boldsymbol{H} \cdot \boldsymbol{\omega})\, \mathrm{d}Y^3 \tag{10}$$

In terms of the finite rotation vector, we may write that $\boldsymbol{\ell} = A_\rho \ddot{\boldsymbol{u}} + \boldsymbol{C}^T \ddot{\boldsymbol{\alpha}}$ and that $\boldsymbol{h} = \boldsymbol{C} \dot{\boldsymbol{u}} + \boldsymbol{\Gamma}^T(\boldsymbol{\alpha}) \boldsymbol{I}_\rho \boldsymbol{\Gamma}(\boldsymbol{\alpha}) \dot{\boldsymbol{\alpha}}$. For simplicity, in the computations we assume the body frame to be a principal axis frame, and hence we take J_α to be zero. Using the definition of adjoint (or transpose) of a vector space operator, we may justify the fact that if the intrinsic wrench[10] $(\boldsymbol{\ell}, \boldsymbol{H})$ is conjugate to the twist[10] $(\dot{\boldsymbol{u}}, \boldsymbol{\omega})$, then $\boldsymbol{h} = \boldsymbol{\Gamma}^T \cdot \boldsymbol{H}$ is conjugate to $\dot{\boldsymbol{\alpha}}$. In fact, in some inner product sense,

denoted by $\langle\cdot\rangle$, it is true that $\langle \boldsymbol{H}, \omega\rangle = \langle \boldsymbol{H}, \boldsymbol{\Gamma}\cdot\dot{\boldsymbol{\alpha}}\rangle = \langle \boldsymbol{\Gamma}^T\cdot\boldsymbol{H}, \dot{\boldsymbol{\alpha}}\rangle = \langle \boldsymbol{h}, \dot{\boldsymbol{\alpha}}\rangle$. By taking the variation of the kinetic energy density of Eq. (10), we also obtain

$$\delta T = \int_L [\ell\cdot\delta^o\boldsymbol{v} + \boldsymbol{H}\cdot\delta^o\omega]\,dY^3 \tag{11}$$

where $\delta^o\boldsymbol{v} = \delta\dot{\boldsymbol{u}} - \varphi_\delta\times\dot{\boldsymbol{u}}$ is the corotational variation of the (absolute) velocity and $\delta^o\omega = \delta\omega - \varphi_\delta\times\omega = \omega_\delta$ is the corotational variation of the angular velocity.[9] Finally, it can be shown that the external virtual work (EVW) may also be written as

$$EVW = \int_L [\boldsymbol{q}\cdot\delta\boldsymbol{u} + \boldsymbol{m}\cdot\varphi_\delta]\,dY^3 \tag{12}$$

where now $\boldsymbol{q}$ and $\boldsymbol{m}$ denote the vector of external forces and external moments distributed along the length of the beam, respectively. For simplicity, distributed moments are not considered.

III. Tangent Inertia Matrices

By taking partial derivatives of the increment of kinetic energy density in terms of the independent variables, described in $\boldsymbol{q}$, we may construct the left-hand side of the Lagrange equations. After some extensive manipulation, and operating with the tangent maps of rotation, we obtain the symmetric tangent inertia matrix

$$\mathcal{M} = \int \begin{pmatrix} A_\rho \boldsymbol{I}_3 & \emptyset \\ \emptyset & \boldsymbol{\Gamma}^T\boldsymbol{I}_\rho\boldsymbol{\Gamma} \end{pmatrix} dY^3 \tag{13}$$

the tangent gyroscopic contribution

$$\mathcal{C} = \int \begin{pmatrix} \emptyset & \emptyset \\ \emptyset & 2\boldsymbol{L}_{\Gamma^T}(\alpha, \boldsymbol{I}_\rho\boldsymbol{\Gamma}\dot{\alpha}) + 2\dot{\boldsymbol{\Gamma}}^T\boldsymbol{I}_\rho\boldsymbol{\Gamma} \end{pmatrix} dY^3 \tag{14}$$

and the tangent centrifugal contribution

$$\mathcal{X} = \int \begin{bmatrix} \emptyset & \emptyset \\ \emptyset & 2\dot{\boldsymbol{L}}_{\Gamma^T}(\boldsymbol{\alpha}, \boldsymbol{I}_\rho\boldsymbol{\Gamma}\dot{\boldsymbol{\alpha}}) + 2\boldsymbol{\Gamma}^T\boldsymbol{I}_\rho\boldsymbol{L}_\Gamma(\boldsymbol{\alpha}, \dot{\boldsymbol{\alpha}}) \end{bmatrix} + \begin{bmatrix} \emptyset & \emptyset \\ \emptyset & \boldsymbol{L}_{\Gamma^T}(\boldsymbol{\alpha}, \boldsymbol{I}_\rho\boldsymbol{\Gamma}\ddot{\boldsymbol{\alpha}}) + \boldsymbol{\Gamma}^T\boldsymbol{I}_\rho\boldsymbol{L}_\Gamma(\boldsymbol{\alpha}, \ddot{\boldsymbol{\alpha}}) \end{bmatrix} dY^3 \tag{15}$$

The residual inertia vector becomes

$$\mathfrak{g} = \int \{\mathcal{M}(\alpha)\cdot\ddot{\boldsymbol{q}} + \mathcal{C}(\alpha, \dot{\alpha})\cdot\dot{\boldsymbol{q}} + \mathcal{K}(\alpha, \dot{\alpha}, \ddot{\alpha})\cdot\boldsymbol{q}\}\,dY^3 \tag{16}$$

Since we assume that deformations are of small magnitude, all integrations are done over the initial length of the element. We can now introduce a finite element interpolation scheme such as $\boldsymbol{q} = \mathcal{N}(Y^3)\boldsymbol{q}_N$, where C^0 linear (two-node) interpolation functions $\mathcal{N}(Y^3)$ are adopted both for the displacement vector and for the finite rotation vector. After interpolation of the nodal variables, the arrays defined earlier can be assembled in the usual way.

IV. Tangent Stiffness Matrix

We use two different approaches to compute the tangent stiffness of the beam element. In the first case, we use a TL corotational approach with a primal, pure displacement-based finite element, in which the incremental variables are referred to the initial configuration. In the second case, we develop a new element that, instead, makes use of a UL point of view and is based on the mixed functional F_3 described earlier, and in which the incremental variables are referred to the previously converged configuration.

A. Corotational Primal Element

The concept of a corotational frame seems to have been introduced by Zaremba in 1903 (Ref. 11). In a general sense, the corotational scheme is just a kinematic split of the deformation gradient into some average rotation tensor $\boldsymbol{E}$ describing the rigid-body motion of the element as a whole and into a part that describes the small deformation. The displacement vector can be additively decomposed into a rigid part and a part caused by deformation.[12–14] The finite rotation vector, instead, cannot be decomposed additively because rotations do not commute. This clarifies the kinematic nature of the corotational decomposition. The choice of $\boldsymbol{E}$ is dependent on what kind of corotational frame one selects, the essential requirement being that $\boldsymbol{E}$ be a strictly orthogonal tensor. The method used to compute the $\boldsymbol{E}$ matrix makes use of the tangent corotational frame, in which the unit vectors s_1 and s_2 lie in the deformed cross section of node P (i.e., are tangent to the deformed cross-section), and the unit vector s_3 completes the right-handed triad. The corotational method is essentially a TL method to describe the kinematics; i.e., the computational observer is always located at the inertial frame. Then, the computational scheme to compute the global tangent consists of three steps. In step 1, the $\boldsymbol{E}$ matrix is computed, and the displacements and rotations associated to each node and caused by deformation only are extracted from the global vectors. In step 2, we compute the tangent stiffness matrix and the residual internal force vector measured with respect to the corotated frame. We implicitly assume that the displacement and rotation vectors caused by deformation are zero at the reference node. Consistently, only a partition of the internal force vector must be used. We have called this procedure the corotational tangent procedure because we make use of the rigidly rotated spatial basis rigidly attached to the cross section of the reference node. A mapping that is similar but that makes use of a projection operator was described in Crisfield[15] and Nour-Omid and Rankin.[16] In step 3, the tangent operators are used to map the local tangent to the global reference frame.

For a two-node element, the internal strain energy can be written as $W_s = W_s(\boldsymbol{d})$, where in symbolic form $\boldsymbol{d} = \boldsymbol{d}(\boldsymbol{D})$ represents the highly nonlinear mapping (because of the rotations) between the local displacements $\boldsymbol{d} = (\boldsymbol{u}_a^e, \boldsymbol{\theta}_a^e)$ of one end of the beam with respect to the other, measured by an observer with respect to a reference point located in the corotational frame, and the global displacements $\boldsymbol{D} = (\boldsymbol{u}_a^g, \boldsymbol{\theta}_a^g, \boldsymbol{u}_b^g, \boldsymbol{\theta}_b^g)$. Defining the internal forces by $\partial W_s/\partial\boldsymbol{d}_a$ and the local tangent matrix by $\partial^2 W_s/\partial\boldsymbol{d}_a\partial\boldsymbol{d}_b$, we may obtain the global vector of internal forces as $(\partial\boldsymbol{d}_i/\partial\boldsymbol{D}_a)^T(\partial W_s/\partial\boldsymbol{d}_i)$ and the global tangent as

$$\mathcal{K}_{ab}^g = \left(\frac{\partial\boldsymbol{d}_a}{\partial\boldsymbol{D}_a}\right)^T\cdot\frac{\partial^2 W_s}{\partial\boldsymbol{d}_a\partial\boldsymbol{d}_b}\cdot\left(\frac{\partial\boldsymbol{d}_b}{\partial\boldsymbol{D}_b}\right) + \sum_{i=1}^{\text{nif}}\frac{\partial}{\partial\boldsymbol{D}_b}\left[\frac{\partial\boldsymbol{d}_i}{\partial\boldsymbol{D}_a}\cdot\frac{\partial W_s}{\partial\boldsymbol{d}_i}\right] \tag{17}$$

where nif is the number of internal forces. We compute the relative rotational deformation of node Q with respect to node P from $\boldsymbol{T}^e(\boldsymbol{\theta}^e) = (\boldsymbol{R}^P)^T\cdot\boldsymbol{R}^Q$ and the relative translational deformation of node Q with respect to node P from $\boldsymbol{u}^e = \boldsymbol{E}^T\cdot\left(\boldsymbol{x}_g^Q - \boldsymbol{x}_g^P\right) - \boldsymbol{X}^e$, and both are measured with respect to the triad at node P. Then, we need to compute the matrix of first partial derivatives $\partial\boldsymbol{d}/\partial\boldsymbol{D}$ and the matrix of second partial derivatives. The computation of these partial derivatives is quite involved, but straightforward, and we refer the reader to Quadrelli.[10]

Then, we consider a thin beam of constant solid cross section and make use of a TL approach by referring the field variables to the initial, undeformed configuration. We introduce the stiffness matrix of the (straight) Timoshenko beam obtained from the variational form of the principle of virtual work, i.e., from F_1, in which the compatibility equations are assumed to be satisfied a priori. The initial stress contribution to the potential energy of the beam can also be written as

$$V_0 = F\int\left[\left(\frac{\partial u_1}{\partial Y^3}\right)^2 + \left(\frac{\partial u_2}{\partial Y^3}\right)^2\right]dY^3 \tag{18}$$

where u_i represent the small displacement components in the local frame. This stiffness matrix is valid for infinitesimal nodal displacements and rotations and may be derived assuming linear shape functions for the axial and torsional deformations, whereas the lateral displacements and the nodal rotations are interpolated with Hermite cubics. However, in our simulations, the shape functions for the shear and rotational terms were modified to include the presence of a shear-correction factor. Since the tangent stiffness is computed in its explicit form, including the shear-corrected terms, no shear-locking problem, typical of displacement-based formulations, arises. To the elastic, shear-corrected, stiffness matrix, we add the contribution to the rotational terms that comes from the initial stress term as a result of the axial force. Other initial stress contributions, typically

the moment resultants and the shear forces, were neglected. This is because most of the nonlinear static response of a thin member (beam) can be attributed to the axial load or bending-stretching coupling. For relatively thin members with closed, solid cross section, the bending-torsional coupling can also be neglected, and the contribution of the shear forces and warping are negligible on account of the moderate aspect ratio (thickness/depth < 5) of the beam. The presence of the shear-correction terms is, in some cases, sufficient to model thick beams. We propose to use this element for arbitrarily large rotations of a spatial beam to be incorporated in a multibody dynamics code. The internal force vector is computed using the elastic stiffness and the vector of local deformations.

B. Tangent Stiffness Derived from F_3

In the second approach, we adopt a more sophisticated method and introduce a mixed variational principle proposed by Iura and Atluri[4] for the analysis of three-dimensional curved beams with finite rotations and finite strains. In this derivation, we include all of the initial stress resultants and moments in the initial stress matrix. Therefore, we capture all of the couplings present in the LMB and AMB equations. We propose to use the same four-field (displacement vector, rotation tensor, material stretches and curvatures, and stress resultant and moments) functional proposed there, namely F_1, but implement the UL version of the incremental functional obtained from F_1 after a contact transformation, also in incremental form, is used. As shown earlier, this is the dual three-field functional F_3, where incremental stretches and curvatures have been eliminated. A derivation based on the weak form of the field equations, using a complementary energy principle, was obtained by Shi and Atluri.[17] However, they considered an initially straight member, they included no bending-stretching coupling, and their analysis is limited to frames. We extend this analysis to relax all of these assumptions, by allowing for an initially curved member, all LMB and AMB coupling terms present, and arbitrarily large rotations. Another advantage of mixed variational principles is that the shear-locking problem is also avoided since mixed weak forms of the balance equations are equivalent to reduced numerical integration. The TL increments of the four independent fields in F_3 can be written, with reference to the initial configuration, as $\boldsymbol{q}^{n+1} = \boldsymbol{q}^n + \Delta\boldsymbol{q}$, $\boldsymbol{T}^{n+1} = \boldsymbol{T}^n + \Delta\boldsymbol{T}$, and $\boldsymbol{M}^{n+1} = \boldsymbol{M}^n + \Delta\boldsymbol{M}$. In the UL approach, the reference is the previously converged configuration C^N. Consequently, $\boldsymbol{q}^n$ is zero, but $\boldsymbol{T}^n$ and $\boldsymbol{M}^n$ are not zero since C^N is equilibrated in the sense of a small residual norm. In addition, any stress measure in C^N coincides with the Cauchy stress tensor, and the deformation gradient in C^N reduces to the identity matrix. Therefore, initial stretches and curvatures are also zero. Whereas any tangent stiffness matrix in the TL approach can be divided into materially elastic tangent, initial stress tangent, and initial displacement tangent, in the UL approach, the initial displacement contribution is zero. This fact leads to a reduced number of operations in the UL approach. The incremental form of the F_1 functional in the UL form is then

$$\begin{aligned}\Delta F_1 = \int_{C^n} \big\{ & \Delta W_s(\boldsymbol{h}, \tilde{\boldsymbol{k}}) \\ & + \Delta\boldsymbol{T} \cdot \left\{ \Delta\boldsymbol{u}_{,3} - \Delta\boldsymbol{h} - \Delta\boldsymbol{R} \cdot \left(\boldsymbol{X}^n_{,3} + \Delta\boldsymbol{h} \right) \right\} \\ & - \boldsymbol{T}^n \cdot \left\{ \Delta\boldsymbol{h} + \Delta\boldsymbol{R} \cdot \left(\boldsymbol{X}^n_{,3} + \Delta\boldsymbol{h} \right) \right\} - \Delta\boldsymbol{q} \cdot \Delta\boldsymbol{u} \\ & + (\boldsymbol{M}^n + \Delta\boldsymbol{M}) \cdot \{ \Delta\boldsymbol{l}_3 - (\boldsymbol{l}_3 + \Delta\boldsymbol{R}) \cdot \Delta\tilde{\boldsymbol{k}} \} \big\} \mathrm{d}Y^3 + BT \end{aligned} \tag{19}$$

where BT are boundary terms, omitted for conciseness. Consequently, we may write the incremental form of the contact transformation as

$$\Delta W_s + \Delta W_c = \Delta\boldsymbol{T} \cdot \Delta\boldsymbol{h} + (\boldsymbol{M}^n + \Delta\boldsymbol{M}) \cdot \Delta\tilde{\boldsymbol{k}} \tag{20}$$

Once the variation has been taken and the kinematic equations have been substituted, we use the inverse constitutive relationship and the incremental contact transformation to obtain the complementary version of the incremental variational statement in UL form. We now introduce the unknown stress parameters $\Delta\varkappa$ at the element level and the nodal displacement and rotation vectors Δq_N as independent fields. Linear trial and test functions are assumed for $\Delta\boldsymbol{q}$, and for the internal stress resultants and moments, which suffices to capture at least the simplest (linear) variation of applied distributed load. After some straightforward algebra, we obtain the discretized incremental variational statement ΔF_3 as

$$\begin{aligned} & \delta(\Delta\varkappa)^T \cdot \{ -\boldsymbol{B} \cdot \Delta\varkappa + \boldsymbol{A} \cdot \Delta\boldsymbol{q} + \boldsymbol{f}_1 \} \\ & \quad + \delta(\Delta\boldsymbol{q}_N)^T \cdot \{ \boldsymbol{C} \cdot \Delta\varkappa + \boldsymbol{D} \cdot \Delta\boldsymbol{q} + \boldsymbol{f}_2 \} = 0 \end{aligned} \tag{21}$$

After condensation, we may eliminate the stress parameter increments at the element level and obtain the stress increments as $\Delta\varkappa = \boldsymbol{B}^{-1}(\boldsymbol{A} \cdot \Delta\boldsymbol{q} + \boldsymbol{f}_1)$ and the tangent stiffness matrix and residual vector, referred to the current configuration, as $\boldsymbol{K} = \boldsymbol{C} \cdot \boldsymbol{B}^{-1}\boldsymbol{A} + \boldsymbol{D}$ and $\boldsymbol{f} = \boldsymbol{C} \cdot \boldsymbol{B}^{-1}\boldsymbol{f}_1 + \boldsymbol{f}_2$. Here, $\boldsymbol{B}$ denotes the elastic compliance matrix, $\boldsymbol{C}$ is the initial stress matrix, $\boldsymbol{D}$ is a geometric transformation matrix, and $\boldsymbol{f}_1$ and $\boldsymbol{f}_2$ are residual vectors. Note that, given the C^0 assumption for the independent fields, several of these integrals may be easily evaluated in closed form. The remaining ones were evaluated with a two-point Gauss quadrature. We add the external loading terms after global assembly has been completed. However, because we deal mainly with conservative loads (i.e., loads whose direction is fixed in the inertial basis), they need to be transformed with the global rotation matrix to the current frame. During the solution procedure, the displacements and rotations are updated as usual, but the stress parameters need to be updated differently. In particular, by means of the incremental rotation tensor from the Nth to the $N+1$st stage, they have to be rotated to the current basis before updating them and obtaining the initial stress parameters for the next increment.

V. Numerical Results

We have selected the implicit Hilber–Hughes–Taylor (HHT)[18] algorithm to integrate in time the tangent equations of motion. The HHT method allows for some tunable degree of artificial viscosity, which is beneficial when kinematic constraints are present.[19] In addition, the unconditional stability characteristics of Newmark's integrator for linear systems are preserved. The tangent iteration matrices are solved for the incremental variables with the Newton–Raphson method until a specified convergence criterion is satisfied. The algorithm may be extended to include, for the static case, a continuation method (arc-length method) able to trace the response in the postbuckling regime. The structure of the system tangent iteration matrix is unsymmetric because the skew-symmetric tangent gyroscopic matrix is also present.

Next we discuss some numerical results obtain using the displacement-based corotational element in TL form (case a) and the mixed element in UL form (case b). Two Gauss points were used for the numerical integration of the integrals involving the tangent inertia matrices. The beam has been discretized using only five corotational elements in case a and with one mixed element in case b. We compare this element discretization with similar results, present in the literature, and which make use of 10 or more elements. The tolerance used was 10^{-8}. The comparisons for the static problems are made with the results presented in Refs. 1, 2, 15, and 20. Figure 2 shows the static behavior of a cantilever beam, looping three times around the clamped point when an end conservative moment is applied, and in which the element undergoes extremely large rotations. The comparison with the exact results obtained by Bishhop and Drucker,[21] depicted in Fig. 3, is excellent. With the tangent corotational method, the result could be obtained in one increment of load, four iterations, and to an accuracy of less than 10^{-10} in the residue norm. However, to show the beam curvature, this plot was obtained with 16 Timoshenko beam elements, including the axial force effect, and with no contribution of the second part of the tangent stiffness matrix. Figure 4 represents the comparison with the theoretical results for the same problem modeled with two elements of the type discussed in case b. Figure 5 represents the same problem modeled with one element of the type discussed in case b. Although Fig. 5 shows only one increment of load, the comparison with the exact solution (continuous line) is excellent, also considering the magnitude of the deformation involved, substantially larger than common deformation patterns encountered in

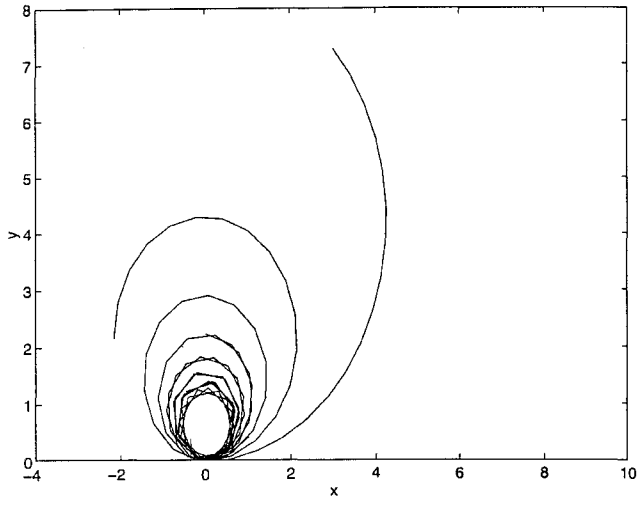

Fig. 2 Cantilever beam with end moment looping three times; TL corotational element.

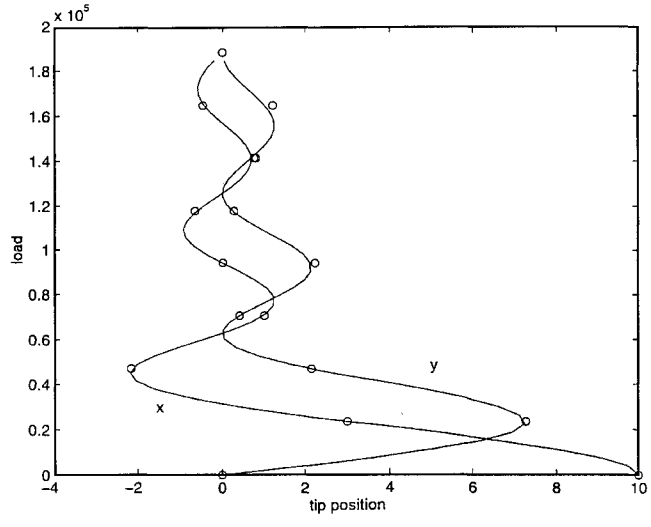

Fig. 3 Cantilever beam with end moment looping three times; TL corotational element. Comparison with exact results.

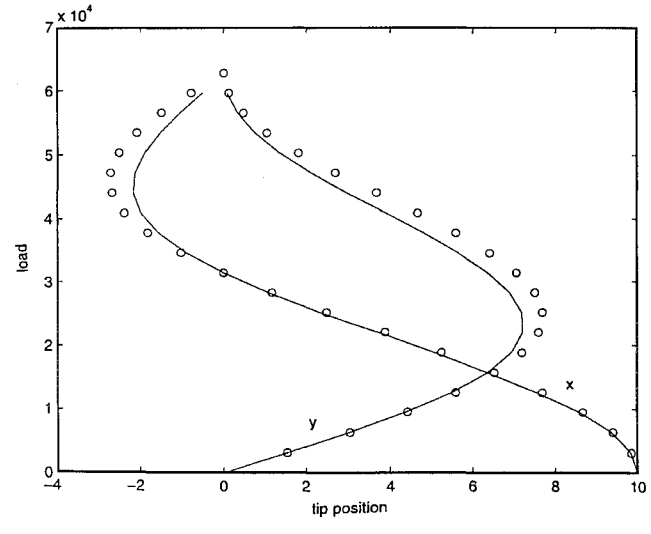

Fig. 4 Cantilever beam with end moment; two UL mixed elements. Comparison with exact results.

Table 1 Comparison of results of 45-deg bend problem

	$f = 300$			$f = 450$			$f = 600$		
Bathe	22.50	59.20	39.50	——	——	——	15.90	47.20	53.40
Simo	22.33	58.84	40.08	18.62	52.32	48.39	15.79	47.23	53.37
Cardona	22.14	58.66	40.65	18.23	51.84	49.31	15.26	46.48	54.54
Crisfield	22.16	58.53	40.53	18.43	51.93	48.79	15.61	46.48	53.71
Present	22.46	59.15	39.75	19.69	52.56	48.31	15.83	47.41	53.43

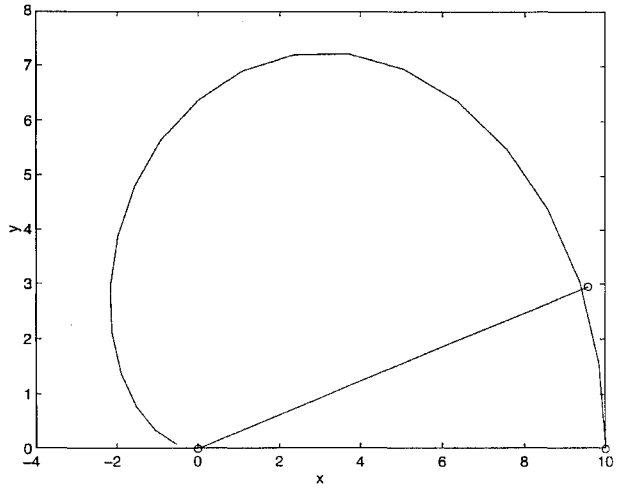

Fig. 5 Cantilever beam with end moment; one UL mixed element.

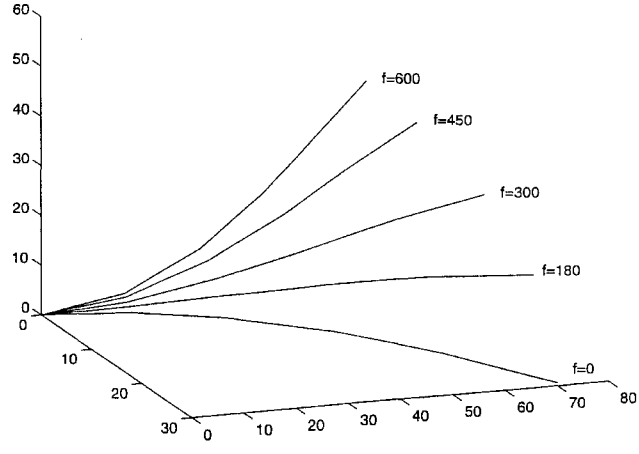

Fig. 6 The 45-deg bend problem.

multiflexible body dynamics. From this result we infer the much superior performance of the mixed method compared with the primal method with five elements per beam. However, a penalty of using only one element for extremely large deformation problems must be paid since this leads to a degradation of convergence properties. Figure 6 shows the behavior of a curved beam bent to form an eighth of a circle in the plane by a force along the z direction. The problem is also known as the 45-deg bend problem. This test is representative of a full three-dimensional response. As shown in Table 1, the comparison with previous results obtained for the same problem by different authors is also excellent. We solved this problem with 10 equal load increments and with an average of 11 iterations per step. Figure 7 depicts a diamond-shaped frame that is also undergoing snapping through. The frame is compressed by two equal forces acting at the two opposite corners along the y axis. This is a postbuckling response case, and we used five elements per side. The comparison with previous results, typically with at least 10 members per side, is also very good. Hence we conclude that this new type of element also performs well in the case of limit

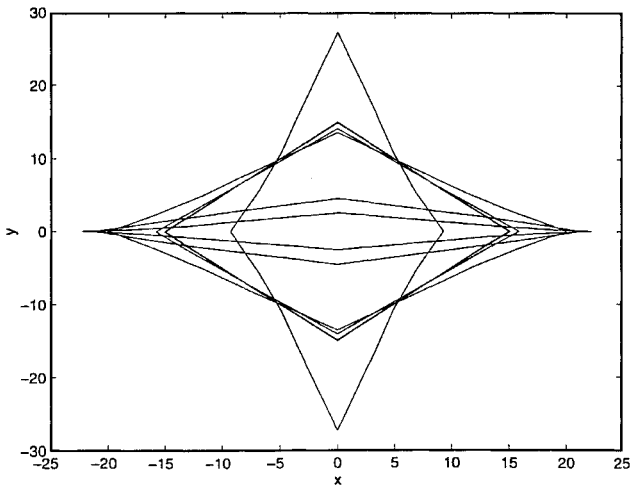

Fig. 7 Postbuckling of diamond-shaped frame.

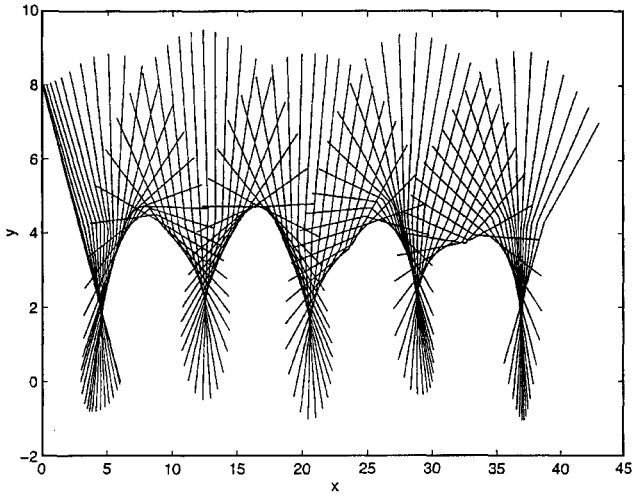

Fig. 8 Free-flying flexible beam; two elements.

point analysis. Figure 8 shows the response of a free-flying beam subjected to a time-dependent conservative force pulse (along the increasing horizontal direction) and to a rectangular torque pulse of 80 Nm acting for 2.5 units of time and acting at the lower tip of the beam. The time step was also taken to be 0.05 units of time. This example is also analyzed in Iura and Atluri,[4] and our results, for multiple revolutions, and with only two elements, compare very well with those reported there. Although large rotations are involved, the average number of iterations per time step in the dynamics problems was three. Convergence was also reached when the full consistent tangent inertia contributions were used. We can then conclude that, for large rotations of three-dimensional problems, the full tangent inertia contributions are required in numerical simulation.

VI. Conclusions

A formulation to simulate the static and dynamic behavior of elastic, geometrically nonlinear beams capable of undergoing arbitrarily large rotations and moderate deformations has been presented. The formulation can be incorporated in a nonlinear finite element code to analyze the dynamic response of multiflexible body systems. To this end, first, the use of the tangent maps of the finite rotation vector to correctly linearize the inertia forces ensures convergence of the incremental/iterative procedure. Second, we introduce the TL tangent corotational method to compute the tangent stiffness matrix of the space beam, obtaining numerical results that compare excellently with theoretical predictions, even in the postbuckling regime. Third, a new element based on the UL form of a mixed variational principle has also been derived and its excellent performance verified for a large deformation problem, with very promising applications in the field of multiflexible body dynamics.

Acknowledgments

The first author would like to thank S. N. Atluri for directing him in this research and H. Lipkin and O. Bauchau for giving him valuable insights into the problem.

References

[1]Simo, J. C., and Vu-Quoc, L., "A Three-Dimensional Finite Strain Rod Model, Part 2: Computational Aspects," *Computer Methods in Applied Mechanics and Engineering*, Vol. 58, No. 1, 1986, pp. 79–116.

[2]Cardona, A., and Geradin, M., "A Beam Finite Element Non-Linear Theory with Finite Rotations," *International Journal for Numerical Methods in Engineering*, Vol. 26, No. 11, 1988, pp. 2403–2438.

[3]Iura, M., and Atluri, S. N., "Dynamic Analysis of Finitely Stretched and Rotated Three-Dimensional Space-Curved Beams," *Computers and Structures*, Vol. 29, No. 5, 1989, pp. 875–889.

[4]Iura, M., and Atluri, S. N., "On a Consistent Theory, and Variational Formulation, of Finitely Stretched and Rotated 3-D Space-Curved Beams," *Computational Mechanics*, Vol. 4, No. 3, 1989, pp. 73–88.

[5]Argyris, J., "An Excursion into Large Rotations," *Computer Methods in Applied Mechanics and Engineering*, Vol. 32, 1982, pp. 85–155.

[6]Pietraszkiewicz, W., and Badur, J., "Finite Rotations in the Description of Continuum Deformation," *International Journal of Engineering Science*, Vol. 21, No. 9, 1983, pp. 1097–1115.

[7]Atluri, S. N., "Alternate Stress and Conjugate Strain Measures, and Mixed Variational Formulations Involving Rigid Rotations, for Computational Analyses of Finitely Deformed Solids, with Application to Plates and Shells—I Theory," *Computers and Structures*, Vol. 18, No. 1, 1984, pp. 98–116.

[8]Atluri, S. N., and Cazzani, A., "Rotations in Computational Solid Mechanics," *Archives of Computational Methods in Engineering, State of the Art Reviews*, Vol. 1, No. 1, 1995, pp. 49–138.

[9]Borri, M., Mello, F., and Atluri, S. N., "Variational Approaches for Dynamics and Time-Finite-Elements: Numerical Studies," *Computational Mechanics*, Vol. 7, No. 1, 1990, pp. 49–76.

[10]Quadrelli, M. B., "Dynamic Analysis of Multi-Flexible Body Systems with Spatial Beams and Finite Rotations," Ph.D. Thesis, School of Aerospace Engineering, Georgia Inst. of Technology, Atlanta, GA, May 1996.

[11]Truesdell, C., and Noll, W., *The Nonlinear Field Theories of Mechanics*, edited by S. Flügge, Vol. 3, Encyclopedia of Physics, Springer–Verlag, Berlin, 1965.

[12]Rankin, C. C., and Brogan, F. A., "An Element Independent Corotational Procedure for the Treatment of Large Rotations," *Journal of Pressure Vessel Technology*, Vol. 108, No. 2, 1986, pp. 165–174.

[13]Belytschko, T., and Schwer, L., "Large Displacement, Transient Analysis of Space Frames," *International Journal for Numerical Methods in Engineering*, Vol. 11, 1977, pp. 65–84.

[14]Geradin, M., and Cardona, A., "Kinematics and Dynamics of Rigid and Flexible Mechanisms Using Finite Elements and Quaternion Algebra," *Computational Mechanics*, Vol. 4, No. 1, 1989, pp. 115–135.

[15]Crisfield, M. A., "A Consistent Corotational Formulation for Nonlinear Three-Dimensional Beam Elements," *Computer Methods in Applied Mechanics and Engineering*, Vol. 81, No. 2, 1990, pp. 131–150.

[16]Nour-Omid, B., and Rankin, C. C., "Finite Rotation Analysis and Consistent Linearization Using Projectors," *Computer Methods in Applied Mechanics and Engineering*, Vol. 93, No. 1, 1991, pp. 353–384.

[17]Shi, G., and Atluri, S. N., "Elasto-Plastic Large Deformation Analysis of Space-Frames: A Plastic-Hinge and Stress-Based Explicit Derivation of Tangent Stiffness," *International Journal for Numerical Methods in Engineering*, Vol. 26, No. 3, 1988, pp. 589–615.

[18]Hilber, H. M., Hughes, T. J. R., and Taylor, R. L., "Improved Numerical Dissipation for Time Integration Algorithms in Structural Dynamics," *Earthquake Engineering and Structural Dynamics*, Vol. 5, 1977, pp. 282–292.

[19]Cardona, A., and Geradin, M., "Numerical Integration of Second Order Differential Algebraic Systems in Flexible Mechanism Dynamics," *Computer-Aided Analysis of Rigid and Flexible Mechanical Systems*, NATO Advanced Study Inst. Series, 1994.

[20]Bathe, K. J., and Bolourchi, S., "Large Displacement Analysis of Three-Dimensional Beam Structures," *International Journal for Numerical Methods in Engineering*, Vol. 14, 1979, pp. 961–986.

[21]Bishhop, K. E., and Drucker, D. C., "Large Deflections of Cantilever Beams," *Quarterly of Applied Mathematics*, Vol. 3, 1945, pp. 272–275.